

A member of the Whirly family is a multifunctional RNA- and DNA-binding protein that is essential for chloroplast biogenesis

Jana Prikryl¹, Kenneth P. Watkins¹, Giulia Friso², Klaas J. van Wijk² and Alice Barkan^{1,*}

¹Institute of Molecular Biology, University of Oregon, Eugene, OR 97405 and ²Department of Plant Biology, Cornell University, Ithaca, NY 14853, USA

Received June 18, 2008; Revised July 14, 2008; Accepted July 16, 2008

ABSTRACT

'Whirly' proteins comprise a plant-specific protein family whose members have been described as DNA-binding proteins that influence nuclear transcription and telomere maintenance, and that associate with nucleoids in chloroplasts and mitochondria. We identified the maize WHY1 ortholog among proteins that coimmunoprecipitate with CRS1, which promotes the splicing of the chloroplast *atpF* group II intron. ZmWHY1 localizes to the chloroplast stroma and to the thylakoid membrane, to which it is tethered by DNA. Genome-wide coimmunoprecipitation assays showed that ZmWHY1 in chloroplast extract is associated with DNA from throughout the plastid genome and with a subset of plastid RNAs that includes *atpF* transcripts. Furthermore, ZmWHY1 binds both RNA and DNA *in vitro*. A severe *ZmWhy1* mutant allele conditions albino seedlings lacking plastid ribosomes; these exhibit the altered plastid RNA profile characteristic of ribosome-less plastids. Hypomorphic *ZmWhy1* mutants exhibit reduced *atpF* intron splicing and a reduced content of plastid ribosomes; aberrant 23S rRNA metabolism in these mutants suggests that a defect in the biogenesis of the large ribosomal subunit underlies the ribosome deficiency. However, these mutants contain near normal levels of chloroplast DNA and RNAs, suggesting that ZmWHY1 is not directly required for either DNA replication or for global plastid transcription.

INTRODUCTION

Plant mitochondrial and chloroplast genomes encode ~50 and ~100 products, respectively, most of which participate in basal organellar gene expression or energy transduction. Post-transcriptional events play the dominant

role in dictating gene product abundance in both organelles (1). In fact, the two organelles house a similar repertoire of RNA-processing pathways that includes RNA editing, group II intron splicing and endonucleolytic processing. Genetic and bioinformatic analyses suggest that many hundreds of nuclear genes encode organelle-localized nucleic acid binding proteins and influence organellar gene expression (2–5), but only a small fraction of such genes has been studied.

The protein that is the focus of this study, ZmWHY1, came to our attention during our characterization of the chloroplast RNA splicing machinery. Nine nucleus-encoded proteins that are necessary for the splicing of various subsets of the ~20 chloroplast introns in vascular plants have been reported (6–15). One of the first to be characterized, CRS1, is necessary for the splicing of the group II intron in the chloroplast *atpF* gene (6,9), and binds specifically to that intron *in vivo* and *in vitro* (10,11,16). However, the large size of the particles containing CRS1 and *atpF* intron RNA *in vivo*, and the fact that CRS1 is not sufficient to promote *atpF* intron splicing *in vitro* suggested that additional proteins are involved. We therefore used mass spectrometry to identify proteins that coimmunoprecipitate with CRS1; ZmWHY1 was one such protein.

ZmWHY1 is a member of the 'Whirly' protein family, whose orthologs in potato (StWHY1) and Arabidopsis (AtWHY1) were reported to be nuclear transcription factors involved in pathogen-induced transcription (17,18). StWHY1 and AtWHY1 bind single-stranded DNA (ssDNA) *in vitro*, and StWHY1 adopts a propeller-like structure from which the family acquired its name (17,19). AtWHY1 has also been implicated in telomere binding and maintenance (20). Additional functions for members of the Whirly family were suggested by the fact that GFP fused to each member of the family from Arabidopsis localizes to chloroplasts or mitochondria (21). The copurification of AtWHY1 with a transcriptionally active chloroplast DNA complex (22) and the association of AtWHY2 with mitochondrial nucleoids (23)

*To whom correspondence should be addressed. Tel: +1 541 346 5145; Fax: +1 541 346 5891; Email: abarkan@uoregon.edu

confirmed that these proteins have organellar functions, but the nature of these functions is not known. Results presented here show that ZmWHY1 plays an essential role in the biogenesis of chloroplasts, that it is associated with DNA from throughout the chloroplast genome and that it interacts *in vivo* with a subset of chloroplast RNAs that includes the *atpF* intron. ZmWHY1 enhances *atpF* intron splicing and influences the biogenesis of the large ribosomal subunit. However, chloroplast DNA and RNAs in *ZmWhy1* mutants accumulate to levels similar to those in other mutants with plastid ribosome deficiencies of similar magnitude. These results argue that ZmWHY1 is required neither for chloroplast DNA replication nor directly for global chloroplast transcription.

MATERIALS AND METHODS

Purification of CRS1 ribonucleoproteins and mass spectrometry

Purification of CRS1 ribonucleoprotein particles and mass spectrometry were performed as described for CAF1 and CAF2 particles in (12). The antibody to CRS1 was described previously (11).

Plant material

Our collection of *Mu* transposon-induced nonphotosynthetic maize mutants (<http://chloroplast.uoregon.edu/>) was screened by PCR to identify insertions in ZmWHY1, using methods described in (24) and a *ZmWhy1*-specific primer (5'-CGGCGGCCTTTCTGGA GGA-3') in conjunction with a *Mu* terminal inverted repeat primer (5'-GCCTCCATTTTCGTCGAATCCCG-3'). The alleles were tested for complementation by crossing phenotypically normal siblings (+/+ or +/-) from ears segregating each allele. Seventy-four ears were recovered, 36 of which segregated chlorophyll-deficient mutants. Other mutants used in this work include *iojap* (25), *hef7* (26) and *crs1* (6). The inbred line B73 (Pioneer HiBred) was used as the source of wild-type tissue for coimmunoprecipitation, sucrose gradient and chloroplast fractionation experiments. Plants were grown in soil in a growth chamber (16 h light, 24°C)/8 h dark, 19°C). Leaf tissue was harvested ~9 days after planting.

Generation of recombinant ZmWHY1 for antibody production and binding assays

ESTs representing *ZmWhy1* were identified as GenBank accessions DV170433 and DV503865; the corresponding cDNAs were obtained from the maize full-length cDNA project (<http://www.maizecdna.org/>). The complete cDNA sequence was determined and has been entered in GenBank under Accession EU595664. A ZmWHY1 protein fragment (amino acids 86 to 258) with a C-terminal 6x-histidine tag was expressed in *Escherichia coli* from pET28b (Novagen), purified by nickel affinity chromatography and used for the production of polyclonal antisera in rabbits at the University of Oregon antibody facility. Full-length mature ZmWHY1 (i.e. lacking the transit peptide) for nucleic acid binding assays was generated by

PCR amplification of its coding sequence from the cDNA (primers 5'-TATAGGATCCGCCTCCTCCCGT AAG-3' and 5'-TATAGTTCGACTCACCGACGCCATT C-3'), digestion of the product with BamHI and Sall, and cloning into pMAL-TEV. Subsequent steps in expressing and purifying recombinant ZmWHY1 were as described previously for RNC1 (12).

Chloroplast fractionation and protein analysis

Leaf protein extracts were prepared and analyzed as previously described (27). Chloroplast subfractions were those described by Williams and Barkan (24). For RNase and DNase treatment of thylakoid membranes, MgCl₂ was added to a thylakoid membrane fraction to a concentration of 15 mM. The sample was divided into three 20 µl aliquots: 1 µl RNase-free RQ1 DNase (1 U/µl) (Promega, Madison, WI, USA), 1 µl of RNase A (1 µg/µl), or 1 µl water was added for the DNase, RNase, and mock treatments, respectively. Samples were incubated at room temperature for 30 min and then centrifuged at 4°C at 15000g for 15 min. The pellet was resuspended in 10 mM Tris-HCl pH 7.5, 2 mM EDTA, 0.2 M sucrose, to a volume equivalent to that of the supernatant. The supernatant and pellet fractions were analyzed by SDS-PAGE and immunoblotting. Sucrose gradient sedimentation of stromal extract was performed as described by Jenkins and Barkan (7); aliquots of stroma were treated with either 3 units RQ1 DNase or 50 µg/ml RNase A for 30 min at room temperature prior to centrifugation. Antisera to spinach chloroplast RPL2 and MDH were generously provided by A. Subramanian (University of Arizona) and Kathy Newton (University of Missouri), respectively. The other antibodies were generated by us and described previously (28).

Nucleic acid coimmunoprecipitation assays

One hundred microliter aliquots of stromal extract (~500 µg of protein) were analyzed by RIP-chip, DIP-chip and slot-blot hybridization using methods described in (29), except that stroma used for RIP-chip assays was treated with DNase prior to immunoprecipitation (10 units RQ1 DNase at 37°C for 30 min) and again after purification of nucleic acids from the immunoprecipitation. For DIP-chip assays, RNase A (100 µg/ml final concentration) was added to stroma prior to immunoprecipitation and residual RNA was removed from the recovered nucleic acids by alkali hydrolysis in 200 mM NaOH at 70°C for 30 min.

Analysis of DNA and RNA

DNA extraction from leaf tissue and Southern blot analysis were performed as previously described (30). Leaf RNA was extracted from the middle of the second leaf of 9-day old seedlings, with Tri Reagent (Molecular Research Center, Cincinnati, OH, USA). RNA gel blot hybridizations were performed as previously described (27). The following PCR fragments were used as probes (residue numbers refer to GenBank accession X86563): *atpF int/ex2*, 35706-36384; *atpF int*, 36073-35233; *ndhA int*, 114941-115730; *orf99*, 86911-88430; *petD ex2*,

75539-75895; *petN*, 19081-19415; *psbA*, 296-1074; *rpl16 ex2*, 79519-79920; *rpl16 int*, 80002-80888; *rpoB*, 23258-24475; *rps12 trans*, 69307-69420 and 129636-129861; *rps12 int1/ex1*, 5', 68793-69460; *rps14*, 38500-39020; *rrn4.5*, 102041-102135; *rrn5*, 102180-102619; *rrn16*, 95559-96779; *rrn23*, 98332-98792; *trnA* mature, 98038-98075 + 98712-98916; *trnG* mature, 13245-13292 and 13991-14013; *trnG int* 13293-13990; *trnN*, 103066-103137; *ycf3 int2/ex3*, 43820-44873; *ycf3 int*, 44383-45116. Poisoned primer extension assays to distinguish mature from precursor RNAs were performed as previously described (9) using the following primers and dideoxynucleotide: *rrn23*, 5'-CGCAAGCCTTTCCTCTTTT-3' (ddTTP); *rpl2*, 5'-GGCCGTGCCTAAGGGCATATC-3' (ddCTP); *rps12*, 5'-GGTTTTTTGGGGTTGATAG-3' (ddCTP). Radioactive gels and blots were imaged with a phosphorimager and analyzed using ImageQuant software (GE Healthcare).

Nucleic acid binding assays

Gel mobility shift assays were performed with the same substrates and procedures as described in Watkins *et al.* (12) except that the binding reactions contained 150 mM NaCl, 5 mM DTT, 50 µg/ml BSA, 25 mM Tris-HCl pH 7.5, 0.1 mg/ml heparin. Filter-binding assays were based on the procedure of Wong and Lohman (31) with modifications (16). The *atpF* intron RNA substrate for filter-binding assays was transcribed *in vitro* by T7 RNA from a PCR product generated with the following primers: *atpF* forward/T7 promoter, 5'-TAATACGACTCACTATAGG GATGAAAAATGTAACCCATTCTT-3'; *atpF* reverse, 5'-AATGAAAGTAGATTATCTTGC-3'. The RNA, which included *atpF* exon 1 and the complete intron, was heated in TE to 90°C for 2 min and then placed on ice immediately prior to its addition to binding reactions (300 mM NaCl, 5 mM DTT, 50 µg/ml BSA and 25 mM Tris pH 7.5, 30°C for 30 min).

Chloroplast run-on transcription assay

The chloroplast run-on transcription assay was performed as described by Mullet and Klein (32–34). The radiolabeled products were hybridized to the following synthetic oligonucleotides (10 pmol/slot) that had been applied with a slot-blot manifold to a nylon membrane: *rrn16* 5'-CC CATTGTAGCACGTGTGTCGCCAGGGCATAAG GGGCATGATGACTTGG-3', *rrn23* 5'-GGACTCTTG GGAAGATCAGCCTGTTATCCCTAGAGTA ACT TTTATCCGA-3', *trnG* 5'-CATCTATGTCAGCTTTTC TGTCTGAATGGAACCAAAGCTCTCCGCTTTCTA GATGC-3' and *CFM3* 5'-ATACTCGAGCGAAAACA GGAGGATTAGTAATCTGGCGATCAGGGACTTC TGTCTCTGTACCGGGGAGTAGATTATGATGA ACC-3'.

RESULTS

Identification of ZmWHY1 in CRS1 coimmunoprecipitates

To find proteins involved in the splicing of the *atpF* intron we used mass spectrometry to identify proteins that coimmunoprecipitate with the *atpF* splicing factor CRS1.

Stromal extract was initially fractionated on a sucrose gradient, and the fractions that contained the majority of the CRS1 ribonucleoprotein particles (~600–700 kDa) were used for immunoprecipitation. The immunoprecipitated proteins were separated by SDS-PAGE, and contiguous gel slices containing proteins between ~20 and ~120 kDa were used for in-gel trypsin digests and tandem mass spectrometry. Among the proteins identified was a member of the Whirly protein family (Supplementary Table 1, Supplementary Figure 1A) (17,19). The Whirly protein family in vascular plants includes two orthologous groups (Supplementary Figure 1B). The peptides detected in the CRS1 coimmunoprecipitate identified the protein as a member of the orthologous group designated Why1.

Recovery of ZmWhy1 insertion mutants

To elucidate the function of ZmWHY1 we sought insertion mutants in a reverse-genetic screen of our collection of transposon-induced non-photosynthetic maize mutants (<http://pml.uoregon.edu/>). Two mutant alleles were recovered (Figure 1): the *Zmwhy1-1* allele has a *MuDR* transposon insertion 35-bp downstream of the predicted start codon and conditions an ivory leaf phenotype; the *Zmwhy1-2* allele has a *Mu1* or *Mu1.7* insertion 38-bp upstream of the predicted start codon and conditions a pale green leaf phenotype. The heteroallelic progeny of complementation crosses (*Zmwhy1-1/-2*) exhibit an intermediate phenotype (Figure 1B). Homozygous mutant plants die after the development of three to four leaves, as is typical of non-photosynthetic maize mutants.

A polyclonal antibody was raised to a recombinant fragment of ZmWHY1. This antibody detected a leaf protein whose size is consistent with that anticipated for ZmWHY1 (~25 kDa) (data not shown) and whose abundance is reduced in *ZmWhy1* mutants (Figure 1C), indicating that the detected protein is ZmWHY1. The ZmWHY1 antibody coimmunoprecipitated CRS1 (Figure 1D) from chloroplast extract, confirming that CRS1 and ZmWHY1 associate with one another. This association was disrupted by treatment with ribonuclease A (Figure 1D), indicating it is mediated by RNA. Results described below show that *atpF* intron RNA, which was shown previously to associate with CRS1 *in vivo* (10,11), mediates the CRS1/ZmWHY1 interaction.

ZmWHY1 partitions between the chloroplast stroma and thylakoid membrane, to which it is bound in a DNA-dependent manner

ZmWHY1 was initially recovered from chloroplast stroma and is predicted to localize to chloroplasts by both the TargetP (35) and Predotar (36) algorithms. Immunoblot analysis of proteins from leaf, chloroplasts and mitochondria confirmed that ZmWHY1 is found in chloroplasts and that it is absent, or found at only very low levels, in mitochondria (Figure 2A). Analysis of chloroplast subfractions showed that ZmWHY1 is recovered in both the stromal and thylakoid membrane fractions (Figure 2A); this behavior differs from that of other chloroplast gene expression factors in the same

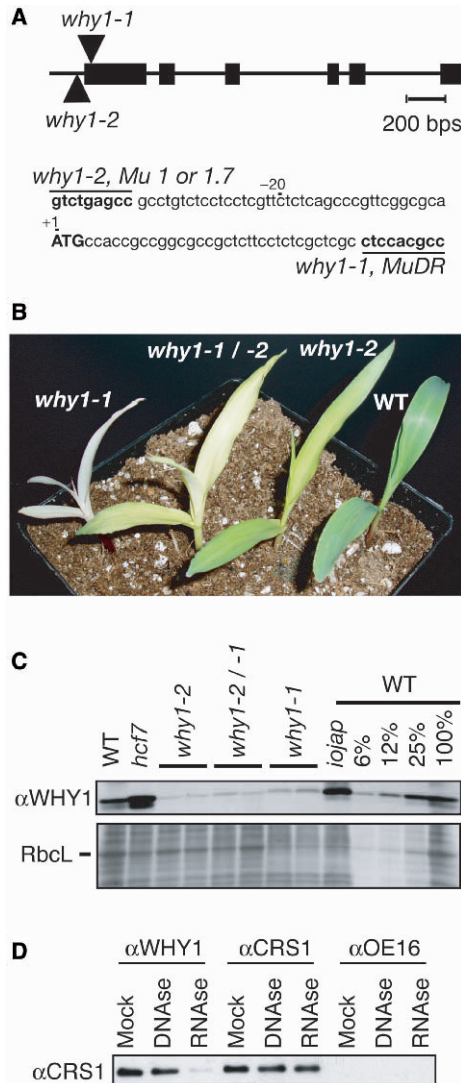


Figure 1. Mutant alleles of *ZmWhy1*. (A) Positions of *Mu* transposon insertions in the *ZmWhy1* gene. Protein coding regions are indicated by rectangles, untranslated regions and introns by lines and *Mu* transposon insertions by triangles. The sequence of each insertion site is shown below, with the nine nucleotides that were duplicated during insertion underlined. The identity of the member of the *Mu* family is shown for each insertion (*why1-2*: Mu1/1.7; *why1-1*: MuDR), and was inferred from polymorphisms in the terminal inverted repeats. (B) Phenotypes of *ZmWhy1* mutant seedlings grown for nine days in soil. Seedlings shown are homozygous for either the *Zmwhy1-1* or *Zmwhy1-2* allele, or are the heteroallelic progeny of a complementation cross. (C) Immunoblot showing loss of *ZmWhy1* in mutant leaf tissue. Total leaf extract (10 μ g protein, or dilutions as indicated) were analyzed. The same blot stained with Ponceau S is shown below, with the large subunit of Rubisco (RbcL) marked. *hcf7* and *iojap* are pale green and albino maize mutants with weak and severe plastid ribosome deficiencies, respectively (25,26). The apparently higher levels of *ZmWhy1* in *Zmwhy1-1* mutants relative to *Zmwhy1-2* mutants may be an artifact of the fact that samples were loaded on the basis of equal total protein: the abundant photosynthetic enzyme complexes make up the bulk of the protein in the *Zmwhy1-2* extract but are missing in the *Zmwhy1-1* extract, causing other proteins to appear over-represented. (D) RNA-dependent coimmunoprecipitation of *ZmWhy1* with CRS1. Prior to immunoprecipitation, stroma was treated with DNase or RNase, or incubated under similar conditions without added nuclease (Mock). The stroma was then subjected to immunoprecipitation with the antibody named at top. Presence of CRS1 in the immunoprecipitation pellets was tested by immunoblot analysis with CRS1 antibody.

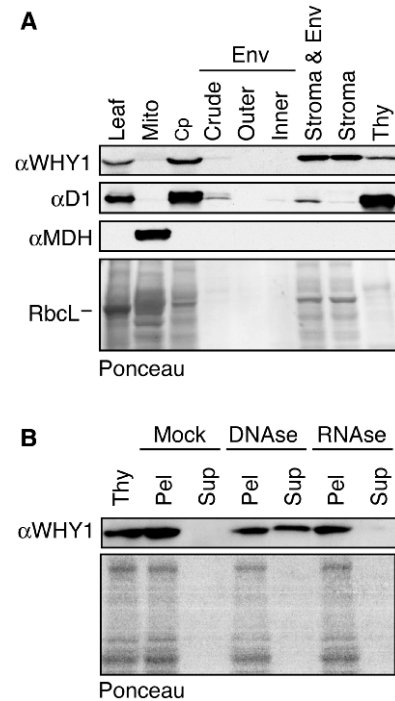


Figure 2. Intracellular localization of *ZmWHY1*. (A) Immunoblots of extracts from leaf and subcellular fractions. The samples in the chloroplast (Cp) and chloroplast subfraction lanes are derived from the same initial number of chloroplasts. The same blot was probed to detect a marker for thylakoid membranes (D1) and mitochondria (MDH). These subcellular fractions are the same as those shown previously for localization of RNC1, where a marker for the envelope membrane fraction was also presented (12). Env; envelope; Mito; mitochondria; Thy; thylakoid membranes. The blot stained with Ponceau S is shown below, with the band corresponding to RbcL marked. (B) DNA-dependent association of *ZmWHY1* with thylakoid membranes. The thylakoid membrane fraction was treated with DNase, RNase or incubated under similar conditions without added nuclease (Mock). Thylakoid membranes were then pelleted by centrifugation. Pellet (Pel) and supernatant (Sup) fractions were brought to equal volumes, and an equivalent proportion of each fraction was analyzed on an immunoblot probed with *ZmWHY1* antibody. The same blot stained with Ponceau S is shown below.

fractionated chloroplast preparation (PPR2, PPR4, RNC1, CAF1, CAF2, CFM2), all of which were found solely in the stromal fraction (8,10,12,15,24).

It seemed possible that *ZmWHY1* associated with the thylakoid membrane via a DNA tether because chloroplast nucleoids are membrane-associated (37) and *AtWHY1* copurified with a chloroplast chromosome preparation (22). In support of this possibility, treatment of the thylakoid membrane fraction with DNase released a portion of the membrane-associated *ZmWHY1* to the soluble fraction (Figure 2B), whereas RNase treatment had no effect. These results indicate that *ZmWHY1* is associated with the thylakoid membrane, at least in part, via an association with chloroplast DNA.

***ZmWHY1* is associated with large RNA- and DNA-containing particles**

The observations that RNase and DNase disrupt *ZmWHY1*'s association with CRS1 and the thylakoid

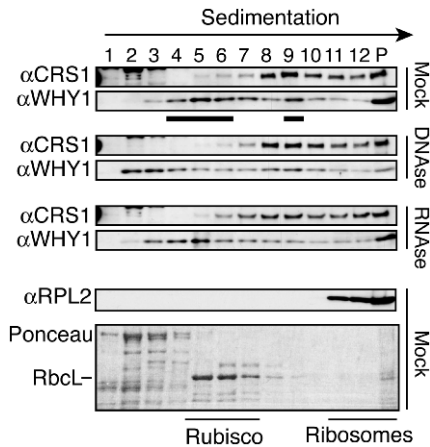


Figure 3. Sucrose-gradient sedimentation demonstrating that ZmWHY1 is associated with DNA- and RNA-containing particles in chloroplast stroma. Stroma extract was treated with DNase or RNase, or incubated under similar conditions without nuclease (Mock), and then sedimented through a sucrose gradient. An equal volume of each gradient fraction was analyzed by probing immunoblots with the antibodies indicated to the left. RPL2, a protein in the large ribosomal subunit, marks the position of ribosomes. Shown below is the blot of the mock-treated fractions stained with Ponceau S, with the RbcL band marked to illustrate the position of Rubisco. The Ponceau S stained blots of experiments involving the DNase- and RNase-treated extracts looked similar (data not shown).

membrane, respectively, suggested that ZmWHY1 associates with both RNA and DNA. To further explore the nature of these interactions, the effects of RNase or DNase treatment on the sedimentation properties of ZmWHY1 were investigated (Figure 3). When untreated stroma was sedimented through a sucrose gradient, ZmWHY1 was detected in two peaks (~400–500 kDa and ~600–700 kDa) and was also found in pelleted material at the bottom of the gradient. The 600–700 kDa peak coincides with the peak of CRS1 in the same gradient. Treatment of stroma with DNase reduced the amount of ZmWHY1 in the pellet and in the ~400–500 kDa peak, but did not reduce its recovery in the 600–700 kDa peak. Conversely, RNase treatment specifically reduced the recovery of ZmWHY1 in the 600–700 kDa peak. These results together with those described above suggested that ZmWHY1 resides in two types of complexes: one that includes CRS1 and RNA, and the other that includes DNA.

Coimmunoprecipitation assays demonstrate that ZmWHY1 associates with a subset of plastid RNAs that includes the *atpF* intron

The RNA-dependent association between ZmWHY1 and CRS1 suggested that ZmWHY1 might associate with CRS1's RNA ligand, the *atpF* intron. However, the albino phenotype conditioned by the *Zmwhy1-1* allele indicated that this could not be ZmWHY1's sole ligand, because mutations in *crs1* that completely block *atpF* intron splicing result in a much less severe chlorophyll deficiency (11). To identify RNAs that associate with ZmWHY1 *in vivo* we used a 'RIP-Chip' assay (38) as an initial screen: RNAs that coimmunoprecipitate with

ZmWHY1 from stromal extract were identified by hybridization to a tiling microarray of the maize chloroplast genome. To ensure that DNA associated with ZmWHY1 did not contribute to the signal, the extract was treated with DNase prior to immunoprecipitation, and the nucleic acids recovered from the immunoprecipitation pellet and supernatant were again treated with DNase. RNAs recovered from the pellet and supernatant were then labeled with red- or green-fluorescing dye, respectively, combined, and hybridized to the microarray. Two replicate immunoprecipitations were analyzed in this manner. To highlight sequences that are enriched in the ZmWHY1 immunoprecipitations, the median enrichment ratio [red(F635)/green (F532)] was plotted according to chromosomal position, after subtracting the median enrichment ratios from control assays (Figure 4A). The results highlight the *atpF* intron as the major RNA ligand of ZmWHY1. The results suggested, in addition, an association between ZmWHY1 and RNAs derived from several other loci (e.g. *rps14*, *rpoC*, *ycf3*, *rps12*, *petD*, *rpl16*, *orf99*). When the same data were analyzed by considering only the signal in the immunoprecipitation pellets, the results were similar (Supplementary Figure 2A).

To validate candidate RNA ligands to emerge from the RIP-chip experiment, RNAs that coimmunoprecipitate with ZmWHY1 were analyzed by slot-blot hybridization using probes corresponding to each RIP-chip peak (Figure 4B). RNAs purified from immunoprecipitations with antibodies to CRS1 and OE16 (a protein that does not bind RNA) were analyzed as controls. As for the RIP-chip assays, the stromal extract was treated with DNase prior to immunoprecipitation and the nucleic acids recovered from the immunoprecipitation were treated again with DNase. The results largely recapitulated the RIP-chip data (see lanes 'R' in Figure 4B): *atpF* intron RNA was confirmed to be strongly enriched in ZmWHY1 immunoprecipitations, whereas RNAs from the *psbA* and *petN* loci, which did not appear as positives in RIP-chip assays, likewise scored negative in the slot-blot hybridization assay. Coimmunoprecipitation with ZmWHY1 was also confirmed for RNAs from the *rps12*, *ndhA*, *rpl16*, *ycf3* and *rps14* loci; as predicted by the RIP-chip data, their degree of enrichment was less than that for the *atpF* intron. However, RNAs from the *petD*, *orf99* and *rrn5* loci, which appeared as minor peaks in the RIP-chip data, did not appear to be enriched based on the slot-blot data; the *orf99* transcript is of very low abundance, however, so it may be enriched in the pellet at levels that are too low to detect. These issues notwithstanding, the RIP-chip and slot-blot hybridization data together show that ZmWHY1 associates with a subset of RNAs in chloroplast extract, and that the *atpF* intron is its major RNA ligand.

DNA from throughout the plastid genome coimmunoprecipitates with ZmWHY1

The effects of DNase-treatment on ZmWHY1's association with the thylakoid membrane (Figure 2B) and on its sedimentation rate (Figure 3) indicated that ZmWHY1 is

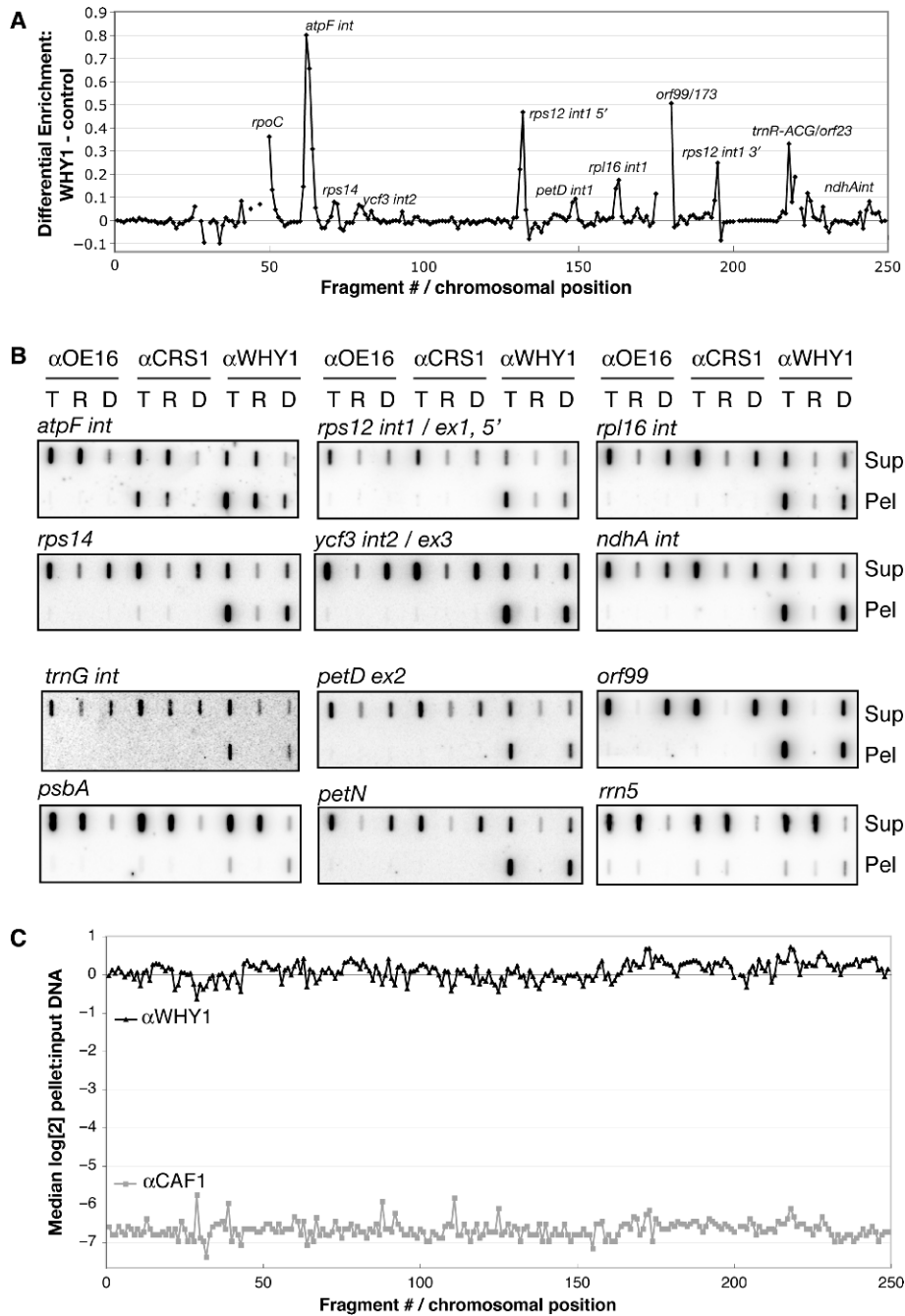


Figure 4. Identification of chloroplast RNAs and DNAs that coimmunoprecipitate with ZmWHY1. (A) RIP-chip data showing coimmunoprecipitation of specific chloroplast RNAs with ZmWHY1. The ratio of signal in the pellet versus the supernatant (F635/F532) for each array fragment is plotted according to chromosomal position. The plot shows the median values for replicate spots across two replicate ZmWHY1 immunoprecipitations after subtracting the corresponding values for two negative control immunoprecipitations (one with OE16 antibody and one without antibody). The same data are plotted using an alternative analysis method in Supplementary Figure 2B; the *atpF* intron is the most prominent peak in both analyses, but the proportional sizes of other peaks vary depending on the comparison used. (B) Validation of RIP-chip and DIP-chip data by slot-blot hybridization. Stroma was pretreated with DNase or RNase or left untreated and then subjected to immunoprecipitation with the antibodies indicated at the top. Nucleic acids purified from the pellets (Pel) and supernatants (Sup) were further treated with DNase or alkali to remove residual DNA or RNA. The resulting total nucleic acids (T), RNA (R) or DNA (D), were applied to a nylon membrane with a slot blot manifold and hybridized with probes specific for the indicated sequences. Slots contained 1/9th or 1/27th of the nucleic acid recovered from each pellet or supernatant, respectively. (C) DIP-chip data showing genome-wide enrichment of chloroplast DNA in ZmWHY1 immunoprecipitations. Stroma was treated with RNase prior to immunoprecipitation. Nucleic acids were extracted from the immunoprecipitation pellets and from total input stroma, and subjected to alkali hydrolysis to remove residual RNA prior to analysis by microarray hybridization. The median log₂-transformed ratio of fluorescence in the pellet versus the input is plotted for replicate array fragments as a function of chromosomal position.

associated with chloroplast DNA *in vivo*. To gain insight into which DNA sequences were involved in these interactions, we modified the RIP-chip protocol to detect coimmunoprecipitating DNA (DIP-chip): stromal extract was treated with ribonuclease prior to the immunoprecipitation, and alkali hydrolysis was used to remove residual RNA after the immunoprecipitation. A control immunoprecipitation used antibody to CAF1, a splicing factor that associates with specific chloroplast intron RNAs *in vivo* (10). Both ZmWHY1 and CAF1 were efficiently immunoprecipitated (Supplementary Figure 2C), but the DIP-chip data were strikingly different (Figure 4C): nearly all of the DNA in the input stromal sample coimmunoprecipitated with ZmWHY1, whereas very little DNA was recovered in CAF1 immunoprecipitations. These results confirm that ZmWHY1 is associated with chloroplast DNA and show further that ZmWHY1 either binds throughout the chloroplast genome, or binds to specific DNA regions and coimmunoprecipitates all other DNA sequences due to their linkage to ZmWHY1-binding sites. Incubation of the extract with various restriction enzymes prior to the immunoprecipitation did not reveal the specific enrichment of any DNA sequences (Supplementary Figure 2B), leading us to favor the interpretation that ZmWHY1 is associated with many sites throughout the chloroplast genome. Nucleic acids recovered from the CAF1 and ZmWHY1 immunoprecipitations were also used as a direct template for PCR (Supplementary Figure 2D). The results support the DIP-Chip data: PCR product was obtained using a variety of chloroplast genome primers from the ZmWHY1 coimmunoprecipitation and not from the CAF1 coimmunoprecipitation.

The enrichment of DNA sequences in ZmWHY1 immunoprecipitations was further confirmed by slot-blot hybridization (Figure 4B). As for the DIP-chip assays, stroma was treated with RNase prior to the immunoprecipitation, and residual RNA was removed by alkali hydrolysis after the immunoprecipitation (Figure 4B, lanes 'D'). Antibody to ZmWHY1 coimmunoprecipitated DNA from all sequences tested, whereas DNA was not detected in either the CRS1 or OE16 immunoprecipitations. The DIP-chip, PCR and slot-blot hybridization data provide strong evidence that ZmWHY1 is associated with chloroplast DNA *in vivo* and that it has many binding sites throughout the genome.

Zm *Why1* mutants are deficient for plastid ribosomes

A role for WHY1 in chloroplast gene expression was suggested by the coimmunoprecipitation of ZmWHY1 with CRS1, RNA and DNA, and by the copurification of AtWHY1 with the plastid transcriptionally active chromosome (22). In support of this possibility, core subunits of the chloroplast ATP synthase, photosystem II, photosystem I, the cytochrome *b₆f* complex and Rubisco accumulate to reduced levels in Zm*Why1* mutants (Figure 5B). The protein deficiencies conditioned by the weak allele combinations (Zm*why1-2/-2* and Zm*why1-1/-2*) resemble those in *hcf7* mutants, which have a reduced content of chloroplast ribosomes (26). These proteins were not

detectable in Zm*why1-1* homozygotes, as in albino *iojap* mutants which lack plastid ribosomes (Figure 5B).

The global loss of photosynthetic enzyme complexes in Zm*Why1* mutants suggested an underlying loss of plastid ribosomes. This possibility was confirmed by RNA gel blot hybridizations, which showed a loss of mature 23S, 4.5S and 16S rRNAs in hypomorphic Zm*Why1* mutants, and an increased accumulation of rRNA precursors (Figure 5A). Chloroplast rRNAs were not detectable in plants homozygous for the null Zm*why1-1* allele, as in albino *iojap* leaves. Whereas *hcf7* mutants show a more severe loss of 16S rRNA than 23S and 4.5S rRNAs, the reverse is true for hypomorphic Zm*Why1* mutants. A dramatic increase in the ratio of 23S rRNA precursors to mature 23S rRNA in these mutants was confirmed with a poisoned-primer extension assay (Supplementary Figure 3C).

Some steps in rRNA processing are dependent upon ribosome assembly in chloroplasts, as in bacteria (15,26,39). The aberrant 23S and 4.5S rRNA processing in Zm*Why1* mutants suggested therefore that ZmWHY1 might promote the expression of a gene needed for the assembly of the large ribosomal subunit (an rRNA or ribosomal protein), with loss of the small ribosomal subunit being a secondary effect. It seemed plausible, for example, that ZmWHY1 might promote processive transcription through the chloroplast *rrn* operon; this would differentially affect the large ribosomal subunit due to the distal position of the genes encoding its rRNA components (23S, 4.5S and 5S rRNA) in the operon (see map in Figure 5A). However, the results of chloroplast run-on transcriptions assays argue against this possibility (Figure 5C): the ratio of polymerase transit through the 23S gene in comparison to the 16S rRNA gene, and the ratio of *rrn* operon transcription in comparison to transcription from a different chloroplast locus (*trnG-UCC*) were similar in wild-type and Zm*why1-1/-2* mutant chloroplasts. Furthermore, the rRNA components of the large ribosomal subunit were not reproducibly enriched in ZmWHY1 coimmunoprecipitates (Figure 4A, Supplementary Figure 2B); this suggests that ZmWHY1 does not interact directly with rRNAs or 50S ribosomal subunits, although such interactions cannot be eliminated based on these negative results. Taken together, these results argue that ZmWHY1 directly impacts the expression of a gene encoding a component of the large ribosomal subunit and/or promotes ribosome assembly. Elucidation of its precise role in this process will require further study.

ZmWHY1 promotes *atpF* intron splicing

The coimmunoprecipitation of ZmWHY1 with the *atpF* splicing factor CRS1 and with RNA from the *atpF* locus suggested that ZmWHY1 might be involved in the splicing of *atpF* pre-mRNA. To test this possibility, *atpF* RNA from Zm*why1* mutants was analyzed by RNA gel blot hybridization (Figure 6). To control for pleiotropic effects of weak and severe plastid ribosome deficiencies, RNAs in pale green (hypomorphic) Zm*why1-2* and Zm*why1-2/-1* mutants were compared to those in *hcf7* mutants,

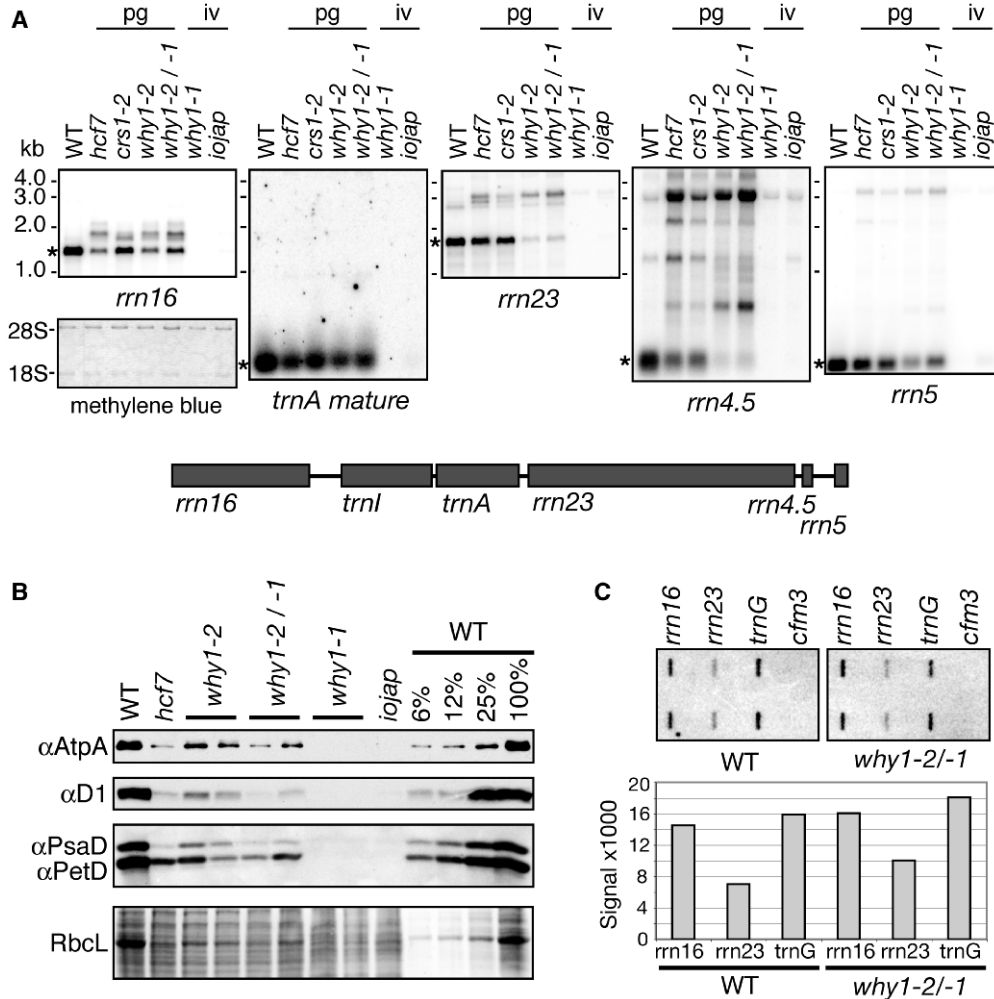


Figure 5. Plastid ribosome deficiency in *ZmWhy1* mutants. (A) Total seedling leaf RNA (0.5 µg) was analyzed by RNA gel blot hybridization using probes for the RNAs indicated at the bottom. A map of the plastid rRNA operon is shown below. A cDNA probe was used to detect mature *trnA*; this lacks intron sequences and therefore hybridizes poorly to unspliced precursor. The probe for 23S rRNA is derived from the 5' portion of the *rnrn23* gene and detects just one of the two 23S rRNA fragments found in ribosomes *in vivo*. The leaf pigmentation conditioned by each mutant allele is indicated: iv: ivory leaves; pg: pale green leaves. The blot used to detect 16S rRNA is shown after staining with methylene blue to illustrate equal loading of cytosolic rRNAs (18S, 28S). Mature RNA forms are indicated with asterisks. (B) Reduced accumulation of photosynthetic enzyme complexes in *ZmWhy1* mutants. Immunoblots of leaf extract (5 µg protein or the indicated dilutions) were probed with antibodies to core subunits of photosynthetic enzyme complexes: AtpA (ATP synthase), D1 (photosystem II), PsalD (photosystem I) and PetD (cytochrome *b6/f* complex). The same blot stained with Ponceau S is shown below to illustrate sample loading and the abundance of RbcL. (C) Plastid runon transcription. Chloroplasts prepared from *Zmwhy1-1/-2* heteroallelic mutants or their normal siblings (wt) were used for runon transcription assays. RNAs purified from the reactions were hybridized to slot blots harboring oligonucleotides corresponding to the genes indicated at the top. Each probe was present in duplicate. *cfm3*, a nuclear gene, served as a negative control. The results were quantified with a phosphorimager and plotted on the bar graph below.

and RNAs in albino (null) *Zmwhy1-1* mutants were compared to those in *iojap* mutants. These comparisons were important because the complete absence of plastid ribosomes in the failure to splice all chloroplast subgroup IIA introns, including the *atpF* intron (6,40,41).

The results in Figure 6 show that the ratio of spliced (S) to unspliced (U) *atpF* transcripts is reduced in hypomorphic *ZmWhy1* mutants in comparison to wild-type and *hcf7* plants, albeit not as severely as in *crs1* mutants. The ratio of excised intron (asterisks) to unspliced RNA is also reduced, supporting the interpretation that *ZmWHY1* promotes *atpF* splicing rather than stabilizing the spliced product. The normal splicing of the *atpF* intron

in *hcf7* mutants argues that the partial plastid ribosome deficiency in hypomorphic *ZmWhy1* mutants cannot account for their reduced *atpF* splicing. Furthermore, a different subgroup IIA intron, the *rpl2* intron, is spliced normally in the same plants (Supplementary Figure 3B), showing that not all subgroup IIA introns are affected in the hypomorphic *ZmWhy1* mutants. These results provide strong evidence that *ZmWHY1*'s association with *atpF* RNA enhances the splicing of the *atpF* intron.

The coimmunoprecipitation data demonstrated an association between *ZmWHY1* and RNAs from several loci other than *atpF*. However, RNA gel blot hybridizations showed that the transcripts from all such genes were

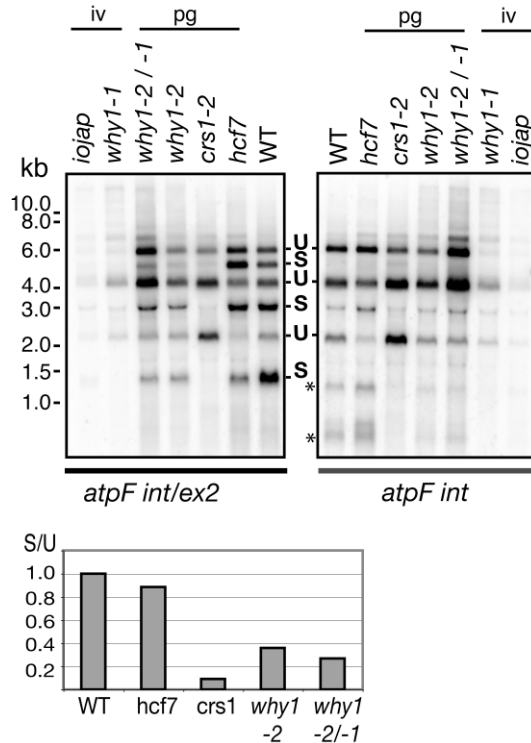


Figure 6. Reduced *atpF* intron splicing in *ZmWhy1* mutants. (A) RNA gel blot analysis of *atpF* splicing. Total seedling leaf RNA (5 µg) was analyzed by RNA gel blot analysis using a probe including *atpF* exon 2 and a portion of the *atpF* intron (*atpF int/ex2*), or with an intron-specific probe (*atpF int*). The *atpF* gene is part of a polycistronic transcription unit that gives rise to a previously characterized population of RNAs (59,60). Spliced (S) and unspliced (U) transcripts are indicated. Asterisks mark bands that we believe correspond to the excised intron and its degradation products. The ratio of spliced to unspliced transcripts was quantified with a phosphorimager, normalized to the wild-type ratio and plotted below using arbitrary units.

qualitatively similar in *ZmWhy1* mutants and in the relevant control mutant (Figure 7). The coimmunoprecipitation of ZmWHY1 with RNAs from both loci encoding the trans-spliced group II intron in *rps12* was intriguing (Figure 4A), but splicing of this RNA is not disrupted in *ZmWhy1* mutants (Supplementary Figure 3B). These results show that ZmWHY1 is not necessary for the normal processing of most chloroplast transcripts.

A structural homolog of ZmWHY1 in *Trypanosoma brucei* is required for mitochondrial RNA editing (42). Several plastid RNAs that are known to be substrates for RNA editing were represented among the RNAs that coimmunoprecipitate with ZmWHY1. Direct sequencing of RT-PCR products demonstrated, however, that the editing of the known edited sites in the *petB*, *rpl20*, *ycf3* and *rps14* transcripts is not disrupted in *Zmwhy1-1* and *Zmwhy1-2/-1* mutants (data not shown), suggesting that ZmWHY1 is not required for RNA editing.

ZmWHY1 is required neither for chloroplast DNA replication nor for global plastid transcription

The association of ZmWHY1 with plastid DNA suggested that it might be involved in chloroplast transcription or

DNA replication. However, Southern blot analysis of total leaf DNA showed that plastid DNA levels in *ZmWhy1* mutants, although somewhat variable from sample to sample, were generally similar to those in normal and control mutant plants (Figure 8). In addition to the plastid transcripts shown in Figure 7, a variety of other transcripts were examined by RNA gel blot hybridization (Supplementary Figure 3A). In no case was a significant reduction in transcript level detected, indicating that ZmWHY1 is not necessary for global plastid transcription. In fact, a trend is apparent toward increased transcript abundance in *ZmWhy1* mutants, but these changes are rather subtle and indirect effects on RNA abundance cannot be excluded.

Recombinant ZmWHY1 binds single-stranded RNA and DNA *in vitro*

To determine whether ZmWHY1 can directly bind both RNA and DNA, recombinant ZmWHY1 (rWHY1) was generated by expression as a maltose-binding protein (MBP) fusion. rWHY1 was released from the MBP moiety by protease cleavage and further purified on a gel filtration column (Figure 9A). rWHY1 eluted from the sizing column at a position corresponding to a globular protein of ~100 kDa, consistent with the report that StWHY1 forms a homotetramer (19). Filter-binding assays showed that rWHY1 binds to unspliced *atpF* RNA *in vitro* (Figure 9B), but it did not show specificity for this RNA relative to other RNAs of similar size under the conditions tested (data not shown).

To compare the affinity of ZmWHY1 for single-stranded and double-stranded RNA and DNA, gel mobility shift assays were used to detect binding to a synthetic 31-mer oligonucleotide in the context of ssDNA, ssRNA, dsDNA or dsRNA (Figure 9C). ZmWHY1 bound rather weakly to these short oligonucleotides but the results showed, nonetheless, that rWHY1 binds both ssDNA and ssRNA, and binds poorly to dsRNA and dsDNA.

DISCUSSION

Previous reports have attributed diverse functions and intracellular locations to WHY1. WHY1 in dicots has been reported to be a ssDNA-binding protein that functions in the nucleus as both a transcription factor (17,19) and as a negative regulator of telomere length (20). Arabidopsis WHY1 copurified with the 'transcriptionally active chromosome' from chloroplasts (22). Our results add another layer to this complex picture. We demonstrate that ZmWHY1 is essential for chloroplast biogenesis, and that it localizes to the chloroplast where it plays multiple roles in gene expression. We also add RNA binding to WHY1's repertoire of biochemical activities and demonstrate that ZmWHY1 is bound to a subset of chloroplast RNAs in chloroplast extract.

Multiple roles of ZmWHY1 in chloroplast biogenesis

ZmWHY was identified among proteins that coimmunoprecipitate with CRS1, which is required for the splicing of the group II intron in the chloroplast *atpF* pre-mRNA.

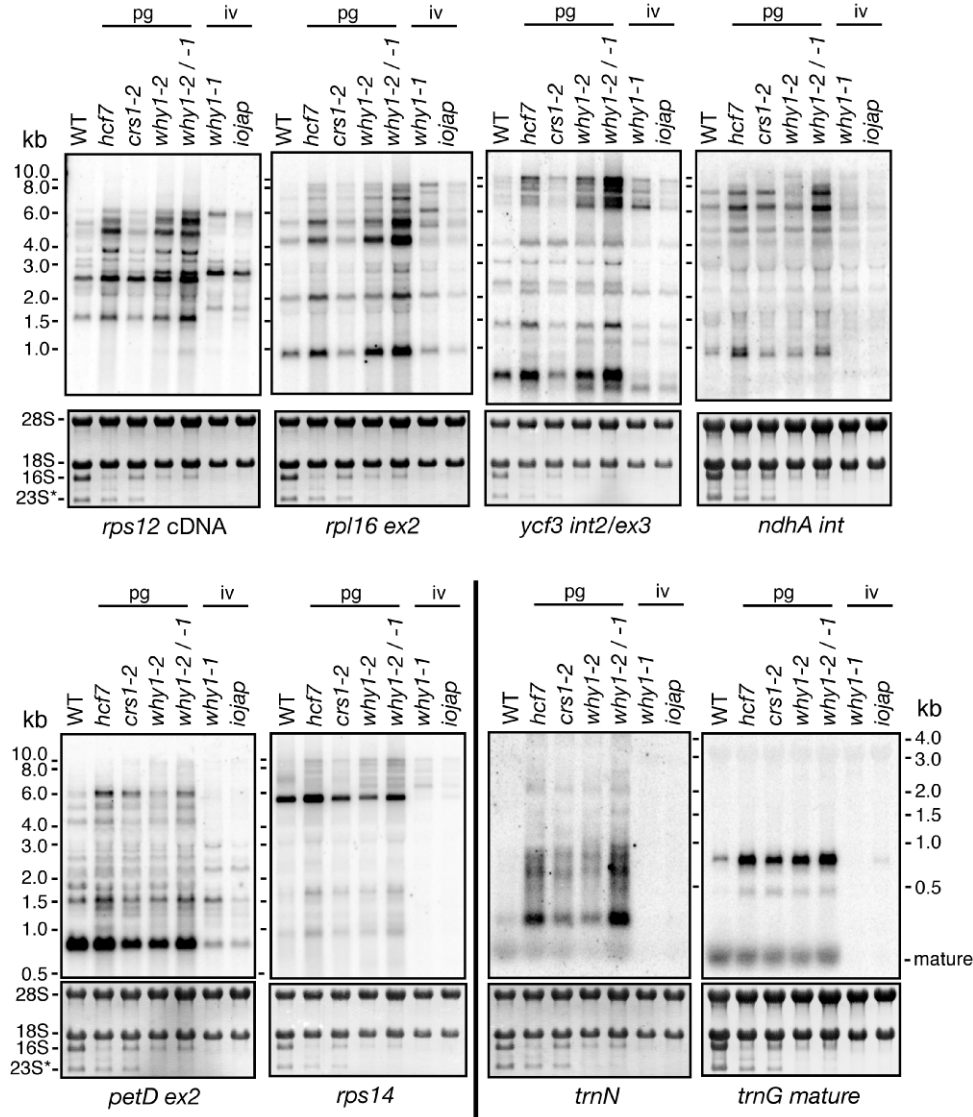


Figure 7. Accumulation of plastid RNAs in *ZmWhy1* mutants. Total seedling leaf RNA (5 μ g) was analyzed by RNA gel blot hybridization using probes specific for the RNAs indicated at bottom. The *rps12* probe was a cDNA probe containing exons 1 and 2. The leaf pigmentation conditioned by each mutant allele is indicated: iv: ivory; pg: pale green. The methylene blue-stained blots are shown below, with rRNAs marked. Additional RNAs that were analyzed analogously are shown in Supplementary Figure 3A.

We showed that ZmWHY1 is associated with *atpF* intron RNA *in vivo* and that the coimmunoprecipitation of ZmWHY1 and CRS1 is disrupted by RNase, indicating that they coimmunoprecipitate due to their association with the same RNA molecule. ZmWHY1's association with *atpF* RNA is functionally significant, as *atpF* intron splicing is disrupted in *ZmWhy1* mutants. However, the splicing of this intron is more sensitive to a partial loss of CRS1 than to a partial loss of ZmWHY1, suggesting that ZmWHY1 plays an accessory function in *atpF* splicing but may not be absolutely required.

The *atpF* splicing defect in *ZmWhy1* mutants cannot account for their loss of plastid ribosomes, as the more severe *atpF* splicing defect in *crs1-1* mutants is not accompanied by a substantial plastid ribosome deficiency (11). The specific role of ZmWHY1 in promoting the biogenesis of the plastid translation machinery remains unclear.

Although several RNAs with translation-related functions are among the RNAs that coimmunoprecipitate with ZmWHY1, the abundance and processing of these RNAs are similar in *ZmWhy1* mutants and in control mutants that exhibit a ribosome-deficiency of similar severity. The specific rRNA deficiencies in *ZmWhy1* mutants do suggest, however, that ZmWHY1 is most directly involved in the biogenesis of the large ribosomal subunit: the accumulation and processing of the 23S and 4.5S rRNAs are more sensitive to the partial loss of *ZmWhy1* function than are those of 16S rRNA, whereas the reverse is true for *hcf7* mutants. Furthermore, in *ppr5* mutants, whose primary defect is in the maturation of a specific plastid tRNA, the rRNAs from the two ribosomal subunits are impacted to a similar extent (39). Thus, our results point to the biogenesis of the plastid large ribosomal subunit as one function of ZmWHY1 but definition of

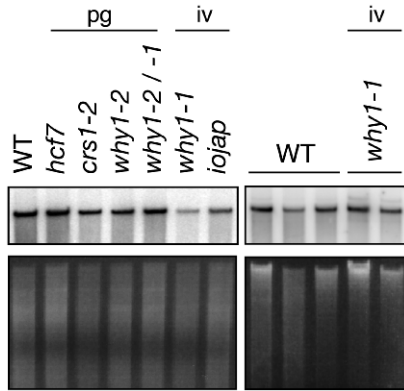


Figure 8. Chloroplast DNA levels in *ZmWhy1* mutants. Seedling leaf DNA (5 μ g) was digested with *EcoRI* (left), or *PvuII* (right) and analyzed by DNA gel blot hybridization using a probe from the chloroplast *rrn23* gene (top left), or *orf99* (top right). The same gels stained with ethidium bromide are shown below. The small fluctuations in relative band intensity may result from small differences in sample loading.

its precise role in this process will require additional study. The strong defect in the processing step that separates 23S rRNA from 4.5S rRNA in hypomorphic *ZmWhy1* mutants is reminiscent of defects reported for mutations in the *DCL*, *DAL* and *RNR1* genes in dicots (43–46). Although it is unclear whether any of these genes function directly in 23S/4.5S rRNA processing, it is possible that *WHY1* acts in concert with one or more of these proteins.

ZmWHY1 binds both RNA and DNA *in vitro* and *in vivo*

We show here that chloroplast DNA coimmunoprecipitates with *ZmWHY1* from plastid extract, that a fraction of *ZmWHY1* is tethered to the thylakoid membrane in a DNA-dependent fashion, that a fraction of stromal *ZmWHY1* is found in DNA-containing particles of ~400 kDa, and that *ZmWHY1* binds ssDNA *in vitro*. These results are consistent with previous reports that dicot *WHY1* binds ssDNA (19,20) and that it copurifies with a chloroplast ‘transcriptionally active chromosome’ (22). Our findings suggest that *ZmWHY1* either binds DNA in a sequence non-specific fashion or that it has many binding sites distributed throughout the plastid genome, because DNA sequences from throughout the plastid genome coimmunoprecipitated to a similar extent with *ZmWHY1*. It remains possible, however, that *ZmWHY1* associates with specific DNA regions *in vivo*, but that these associations were disrupted during lysate preparation. A DNA immunoprecipitation experiment was recently reported for *AtWHY2*, a mitochondrial-localized Whirly protein (23), with analogous results: DNA sequences from a variety of regions throughout the mitochondrial genome coimmunoprecipitated with *AtWHY2*, when assayed by PCR.

We demonstrate here that *ZmWHY1* interacts not only with DNA, as anticipated by previous reports, but that it also binds RNA *in vivo* and *in vitro*. That *ZmWHY1* interacts with RNA is, perhaps, not surprising given that a structural homolog of *ZmWHY1* has been shown to

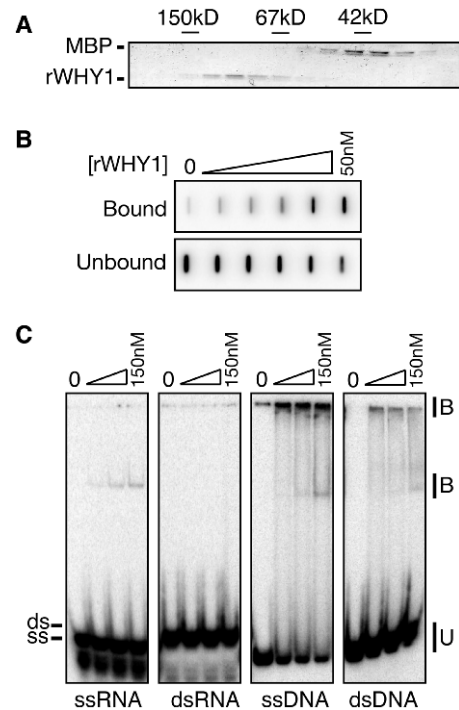


Figure 9. Recombinant *ZmWHY1* binds ssRNA and DNA. (A) Elution of recombinant *ZmWHY1* from a gel filtration column. MBP-WHY1 was purified by amylose affinity chromatography, cleaved with TEV protease to separate the *WHY1* and MBP moieties, and applied to a Superdex 200 column. Column fractions were analyzed by SDS-PAGE and staining with Coomassie blue. The elution position of size markers (alcohol dehydrogenase, 150 kDa; BSA, 67 kDa; MBP, 42 kDa) is shown. The peak *WHY1* fractions were pooled and used for *in vitro* assays. (B) Filter binding assay showing RNA binding activity of *ZmWHY1*. Assays containing 10 pM radiolabeled *atpF* intron RNA and increasing *ZmWHY1* concentrations (50 nM maximum) were filtered through sandwiched nitrocellulose and nylon membranes. Protein-RNA complexes were captured on the nitrocellulose (bound); unbound RNA was captured on the nylon membrane below. (C) Gel mobility shift assay showing *rWHY1*'s relative affinity for double- and single-stranded RNA and DNA. A 31-mer oligonucleotide in RNA or DNA form was radiolabeled, heated and, either snap cooled (ssRNA, ssDNA) or cooled slowly in the presence of monovalent salts and a two-fold excess of its complement (dsRNA, dsDNA). The substrate (40 pM) was mixed with increasing concentrations of *ZmWHY1* (17, 50 and 150 nM). Protein binding is illustrated by the appearance of an upper band and retention at the top of the gel, and by the disappearance of unbound substrate.

bind RNAs involved in kinetoplastid RNA editing (42), and that many proteins that bind ssDNA also bind RNA. The *atpF* intron RNA was the major RNA ligand of *ZmWHY1* detected in the RNA coimmunoprecipitation assays. This RNA is not particularly abundant *in vivo* so its enrichment in *ZmWHY1* immunoprecipitations likely reflects a specific interaction *in vivo*. Although intrinsic specificity for this RNA did not emerge from *in vitro* binding assays using the entire intron, a high-affinity site within a large RNA such as the *atpF* intron (~800 nt) can be masked *in vitro* due to the overwhelming number of nonspecific sites available for protein binding. Therefore, more detailed studies involving smaller RNA ligands will be required to determine whether *ZmWHY1* binds RNA with sequence-specificity or whether it is

recruited to the *atpF* intron via protein–protein interactions.

What is WHY1's DNA-related function in the chloroplast?

The association of ZmWHY1 with DNA sequences from throughout the chloroplast genome suggests that it participates in transcription and/or DNA metabolism. However, our results argue against a general role in transcription, as all plastid mRNAs examined accumulate in hypomorphic *Zmwhy1* mutants to levels that are comparable to those in the relevant control mutants. The results of chloroplast transcription runon experiments argue that the preferential loss of 23S rRNA in these mutants is due to aberrant ribosome assembly rather than to reduced rRNA transcription rates. It remains possible, however, that ZmWHY1 does play a role in chloroplast transcription but that another gene with a partially redundant function serves this purpose in *ZmWhy1* mutants.

It is intriguing that ZmWHY1 binds preferentially to DNA in single stranded form because opportunities to interact with ssDNA *in vivo* are expected to be limited. DNA replication, recombination and repair involve the transient occurrence of ssDNA, and torsional stress can induce DNA unwinding. The Southern blot data showing that plastid DNA levels are no more than minimally decreased in *ZmWhy1* null mutants argue against a central role for ZmWHY1 in DNA replication; however participation of ZmWHY1 in DNA recombination or repair remains possible. In fact, the participation of an unrelated ssDNA-binding protein, OSB1, in plant mitochondrial DNA recombination was reported recently (47).

There are several parallels between our findings with ZmWHY1 and the activities reported for the bacterial protein HU. HU is associated with the bacterial nucleoid, binds preferentially to DNA with irregular structural features (e.g. single stranded gaps and bulges), and is involved in DNA recombination and repair (48,49). Despite its high conservation in bacteria and the presence of an HU homolog in a plastid genome in red algae (50), HU homologs are not encoded in the nuclear or plastid genomes of vascular plants (50,51). Thus, alternative proteins have presumably been recruited in vascular plants to fulfill the functions performed by HU in the chloroplast's cyanobacterial ancestor. The nucleoid-associated protein sulfite reductase has been suggested to be one such protein (51–53), and perhaps WHY1 is another. HU influences global transcription patterns through its effect on nucleoid architecture, and mediates the formation of DNA loops that repress transcription from specific genes (54–56). HU is also an RNA-binding protein, and functions *in vivo* to repress the translation of the *E. coli rpoS* mRNA (57,58). Like HU, ZmWHY1 interacts globally with plastid DNA, but specifically with certain plastid RNAs, and binds preferentially to nucleic acids with single-stranded character. The abundance of several chloroplast mRNAs is increased in *ZmWhy1* mutants, consistent with a global repressive role for ZmWHY1 in transcription. This possibility is in accord with the recent report that over-expression of AtWHY2 in Arabidopsis causes a reduction in the levels of several mitochondrial RNAs (23). Although its role in

DNA metabolism remains uncertain, our results demonstrate that description of WHY1 as a chloroplast transcription factor is, at best, an over-simplification of the complex roles played by this interesting protein.

SUPPLEMENTARY DATA

Supplementary Data are available at NAR Online.

ACKNOWLEDGEMENTS

We thank Rosalind Williams-Carrier for her participation in the purification of CRS1-associated proteins for mass spectrometry, Susan Belcher for maintaining and propagating the mutant lines, and Tiffany Kroeger and Amy Cooke for identifying *ZmWhy1* mutants. We are also grateful to Christian Schmitz-Linneweber for overseeing the sequencing of *ZmWhy1* cDNAs. This work was supported by grants to A.B. (DBI-0421799 and MCB-0314597) and K.J.v.W. (DBI-0211935) from the National Science Foundation. Funding to pay the Open Access publication charges for this article was provided by NSF grant DBI-0421799.

Conflict of interest statement. None declared.

REFERENCES

- Marchfelder,A. and Binder,S. (2004) Plastid and plant mitochondrial RNA processing and RNA stability. In Daniell,H. and Chase,C. (eds), *Molecular Biology and Biotechnology of Plant Organelles*, Kluwer Academic Publishers, Dordrecht, The Netherlands, pp. 261–294.
- Lurin,C., Andres,C., Aubourg,S., Bellaoui,M., Bitton,F., Bruyere,C., Caboche,M., Debast,C., Gualberto,J., Hoffmann,B. *et al.* (2004) Genome-wide analysis of Arabidopsis pentatricopeptide repeat proteins reveals their essential role in organelle biogenesis. *Plant Cell*, **16**, 2089–2193.
- Barkan,A., Klipcan,L., Ostersetzer,O., Kawamura,T., Asakura,Y. and Watkins,K. (2007) The CRM domain: an RNA binding module derived from an ancient ribosome-associated protein. *RNA*, **13**, 55–64.
- Nickelsen,J. (2003) Chloroplast RNA-binding proteins. *Curr. Genet.*, **43**, 392–399.
- Schwacke,R., Fischer,K., Ketelsen,B., Krupinska,K. and Krause,K. (2007) Comparative survey of plastid and mitochondrial targeting properties of transcription factors in Arabidopsis and rice. *Mol. Genet. Genomics*, **277**, 631–646.
- Jenkins,B., Kulhanek,D. and Barkan,A. (1997) Nuclear mutations that block group II RNA splicing in maize chloroplasts reveal several intron classes with distinct requirements for splicing factors. *Plant Cell*, **9**, 283–296.
- Jenkins,B. and Barkan,A. (2001) Recruitment of a peptidyl-tRNA hydrolase as a facilitator of group II intron splicing in chloroplasts. *EMBO J.*, **20**, 872–879.
- Asakura,Y. and Barkan,A. (2007) A CRM domain protein functions dually in group I and group II intron splicing in land plant chloroplasts. *Plant Cell*, **19**, 3864–3875.
- Asakura,Y. and Barkan,A. (2006) Arabidopsis orthologs of maize chloroplast splicing factors promote splicing of orthologous and species-specific group II introns. *Plant Physiol.*, **142**, 1656–1663.
- Ostheimer,G., Williams-Carrier,R., Belcher,S., Osborne,E., Gierke,J. and Barkan,A. (2003) Group II intron splicing factors derived by diversification of an ancient RNA binding module. *EMBO J.*, **22**, 3919–3929.
- Till,B., Schmitz-Linneweber,C., Williams-Carrier,R. and Barkan,A. (2001) CRS1 is a novel group II intron splicing factor that was derived from a domain of ancient origin. *RNA*, **7**, 1227–1238.

12. Watkins, K., Kroeger, T., Cooke, A., Williams-Carrier, R., Friso, G., Belcher, S., Wijk, K.v. and Barkan, A. (2007) A ribonuclease III domain protein functions in group II intron splicing in maize chloroplasts. *Plant Cell*, **19**, 2606–2623.
13. Asakura, Y., Bayraktar, O. and Barkan, A. (2008) Two CRM protein subfamilies cooperate in the splicing of group IIB introns in chloroplasts. *RNA* (in press).
14. Falcon de Longevialle, A., Hendrickson, L., Taylor, N., Delannoy, E., Lurin, C., Badger, M., Millar, A.H. and Small, I. (2008) The pentatricopeptide repeat gene OTP51 with two LAGLIDADG motifs is required for the cis-splicing of plastid ycf3 intron 2 in *Arabidopsis thaliana*. *Plant J.* (in press).
15. Schmitz-Linneweber, C., Williams-Carrier, R.E., Williams-Voelker, P.M., Kroeger, T.S., Vichas, A. and Barkan, A. (2006) A pentatricopeptide repeat protein facilitates the trans-splicing of the maize chloroplast rps12 Pre-mRNA. *Plant Cell*, **18**, 2650–2663.
16. Ostersetzer, O., Watkins, K., Cooke, A. and Barkan, A. (2005) CRS1, a chloroplast group II intron splicing factor, promotes intron folding through specific interactions with two intron domains. *Plant Cell*, **17**, 241–255.
17. Desveaux, D., Subramaniam, R., Despres, C., Mess, J.N., Levesque, C., Fobert, P.R., Dangl, J.L. and Brisson, N. (2004) A “Whirly” transcription factor is required for salicylic acid-dependent disease resistance in *Arabidopsis*. *Dev. Cell*, **6**, 229–240.
18. Desveaux, D., Despres, C., Joyeux, A., Subramaniam, R. and Brisson, N. (2000) PBF-2 is a novel single-stranded DNA binding factor implicated in PR-10a gene activation in potato. *Plant Cell*, **12**, 1477–1489.
19. Desveaux, D., Allard, J., Brisson, N. and Sygusch, J. (2002) A new family of plant transcription factors displays a novel ssDNA-binding surface. *Nat. Struct. Biol.*, **9**, 512–517.
20. Yoo, H.H., Kwon, C., Lee, M.M. and Chung, I.K. (2007) Single-stranded DNA binding factor AtWHY1 modulates telomere length homeostasis in *Arabidopsis*. *Plant J.*, **49**, 442–451.
21. Krause, K., Kilbiński, I., Mulisch, M., Rodiger, A., Schafer, A. and Krupinska, K. (2005) DNA-binding proteins of the Whirly family in *Arabidopsis thaliana* are targeted to the organelles. *FEBS Lett.*, **579**, 3707–3712.
22. Pfalz, J., Liere, K., Kandlbinder, A., Dietz, K.J. and Oelmüller, R. (2006) pTAC2, -6, and -12 are components of the transcriptionally active plastid chromosome that are required for plastid gene expression. *Plant Cell*, **18**, 176–197.
23. Marechal, A., Parent, J.S., Sabar, M., Veronneau-Lafortune, F., Abou-Rached, C. and Brisson, N. (2008) Overexpression of mtDNA-associated AtWhy2 compromises mitochondrial function. *BMC Plant Biol.*, **8**, 42.
24. Williams, P. and Barkan, A. (2003) A chloroplast-localized PPR protein required for plastid ribosome accumulation. *Plant J.*, **36**, 675–686.
25. Walbot, V. and Coe, E.H. (1979) Nuclear gene *iojap* conditions a programmed change to ribosome-less plastids in *Zea mays*. *Proc. Natl Acad. Sci. USA*, **76**, 2760–2764.
26. Barkan, A. (1993) Nuclear mutants of maize with defects in chloroplast polysome assembly have altered chloroplast RNA metabolism. *Plant Cell*, **5**, 389–402.
27. Barkan, A. (1998) Approaches to investigating nuclear genes that function in chloroplast biogenesis in land plants. *Methods Enzymol.*, **297**, 38–57.
28. Voelker, R. and Barkan, A. (1995) Nuclear genes required for post-translational steps in the biogenesis of the chloroplast cytochrome *b6f* complex. *Molec. Gen. Genet.*, **249**, 507–514.
29. Barkan, A. (2008) Genome-wide analysis of RNA-protein interactions in plants. In Belostotsky, D. (ed.), *Plant Systems Biology, Series: Methods in Molecular Biology*, Totowa, NJ, Humana Press.
30. Voelker, R., Mendel-Hartvig, J. and Barkan, A. (1997) Transposon-disruption of a maize nuclear gene, *tha1*, encoding a chloroplast SecA homolog: *in vivo* role of cp-SecA in thylakoid protein targeting. *Genetics*, **145**, 467–478.
31. Wong, I. and Lohman, T. (1993) A double-filter method for nitrocellulose-filter binding: application to protein-nucleic acid interactions. *Proc. Natl Acad. Sci. USA*, **90**, 5428–5432.
32. Mullet, J. and Klein, R. (1987) Transcription and RNA stability are important determinants of higher plant chloroplast RNA levels. *EMBO J.*, **6**, 1571–1579.
33. Rapp, J.C., Baumgartner, B.J. and Mullet, J. (1992) Quantitative analysis of transcription and RNA levels of 15 barley chloroplast genes: transcription rates and mRNA levels vary over 300-fold; predicted mRNA stabilities vary 30-fold. *J. Biol. Chem.*, **267**, 21404–21411.
34. Klein, R. and Mullet, J. (1990) Light-induced transcription of chloroplast genes. *J. Biol. Chem.*, **265**, 1895–1902.
35. Emanuelsson, O. and Heijne, G.v. (2001) Prediction of organellar targeting signals. *Biochim. Biophys. Acta*, **1541**, 114–119.
36. Small, I., Peeters, N., Legeai, F. and Lurin, C. (2004) Predotar: A tool for rapidly screening proteomes for N-terminal targeting sequences. *Proteomics*, **4**, 1581–1590.
37. Sato, N., Terasawa, K., Miyajima, K. and Kabeya, Y. (2003) Organization, developmental dynamics, and evolution of plastid nucleoids. *Int. Rev. Cytol.*, **232**, 217–262.
38. Schmitz-Linneweber, C., Williams-Carrier, R. and Barkan, A. (2005) RNA immunoprecipitation and microarray analysis show a chloroplast pentatricopeptide repeat protein to be associated with the 5'-region of mRNAs whose translation it activates. *Plant Cell*, **17**, 2791–2804.
39. Beick, S., Schmitz-Linneweber, C., Williams-Carrier, R., Jensen, B. and Barkan, A. (2008) The pentatricopeptide repeat protein PPR5 stabilizes a specific tRNA precursor in maize chloroplasts. *Mol. Cell Biol.* (in press).
40. Hess, W.R., Hoch, B., Zeltz, P., Huebschmann, T., Koessel, H. and Boerner, T. (1994) Inefficient *rpl2* splicing in barley mutants with ribosome-deficient plastids. *Plant Cell*, **6**, 1455–1465.
41. Vogel, J., Boerner, T. and Hess, W. (1999) Comparative analysis of splicing of the complete set of chloroplast group II introns in three higher plant mutants. *Nucleic Acids Res.*, **27**, 3866–3874.
42. Schumacher, M.A., Karamoos, E., Zikova, A., Trantirek, L. and Lukes, J. (2006) Crystal structures of *T. brucei* MRP1/MRP2 guide-RNA binding complex reveal RNA matchmaking mechanism. *Cell*, **126**, 701–711.
43. Bollenbach, T.J., Lange, H., Gutierrez, R., Erhardt, M., Stern, D.B. and Gagliardi, D. (2005) RNR1, a 3'-5' exoribonuclease belonging to the RNR superfamily, catalyzes 3' maturation of chloroplast ribosomal RNAs in *Arabidopsis thaliana*. *Nucleic Acids Res.*, **33**, 2751–2763.
44. Bellaoui, M., Keddie, J.S. and Gruissem, W. (2003) DCL is a plant-specific protein required for plastid ribosomal RNA processing and embryo development. *Plant Mol. Biol.*, **53**, 531–543.
45. Bellaoui, M. and Gruissem, W. (2004) Altered expression of the *Arabidopsis* ortholog of DCL affects normal plant development. *Planta*, **219**, 819–826.
46. Bisanz, C., Begot, L., Carol, P., Perez, P., Bligny, M., Pesey, H., Gallois, J.L., Lerbs-Mache, S. and Mache, R. (2003) The *Arabidopsis* nuclear DAL gene encodes a chloroplast protein which is required for the maturation of the plastid ribosomal RNAs and is essential for chloroplast differentiation. *Plant Mol. Biol.*, **51**, 651–663.
47. Zaegel, V., Guermann, B., Le Ret, M., Andres, C., Meyer, D., Erhardt, M., Canaday, J., Gualberto, J.M. and Imbault, P. (2006) The plant-specific ssDNA binding protein OSB1 is involved in the stoichiometric transmission of mitochondrial DNA in *Arabidopsis*. *Plant Cell*, **18**, 3548–3563.
48. Dorman, C.J. and Deighan, P. (2003) Regulation of gene expression by histone-like proteins in bacteria. *Curr. Opin. Genet. Dev.*, **13**, 179–184.
49. Kamashev, D., Balandina, A., Mazur, A.K., Arimondo, P.B. and Rouviere-Yaniv, J. (2008) HU binds and folds single-stranded DNA. *Nucleic Acids Res.*, **36**, 1026–1036.
50. Kobayashi, T., Takahara, M., Miyagishima, S.Y., Kuroiwa, H., Sasaki, N., Ohta, N., Matsuzaki, M. and Kuroiwa, T. (2002) Detection and localization of a chloroplast-encoded HU-like protein that organizes chloroplast nucleoids. *Plant Cell*, **14**, 1579–1589.
51. Sato, N. (2001) Was the evolution of plastid genetic machinery discontinuous? *Trends Plant Sci.*, **6**, 151–55.
52. Sato, N., Nakayama, M. and Hase, T. (2001) The 70-kDa major DNA-compacting protein of the chloroplast nucleoid is sulfite reductase. *FEBS Lett.*, **487**, 347–350.
53. Sekine, K., Fujiwara, M., Nakayama, M., Takao, T., Hase, T. and Sato, N. (2007) DNA binding and partial nucleoid localization of the chloroplast stromal enzyme ferredoxin:sulfite reductase. *FEBS J.*, **274**, 2054–2069.

54. Lia,G., Bensimon,D., Croquette,V., Allemand,J.F., Dunlap,D., Lewis,D.E., Adhya,S. and Finzi,L. (2003) Supercoiling and denaturation in Gal repressor/heat unstable nucleoid protein (HU)-mediated DNA looping. *Proc. Natl Acad. Sci. USA*, **100**, 11373–11377.
55. Kar,S., Edgar,R. and Adhya,S. (2005) Nucleoid remodeling by an altered HU protein: reorganization of the transcription program. *Proc. Natl Acad. Sci. USA*, **102**, 16397–16402.
56. Lewis,D.E., Geanakopoulos,M. and Adhya,S. (1999) Role of HU and DNA supercoiling in transcription repression: specialized nucleoprotein repression complex at gal promoters in *Escherichia coli*. *Mol. Microbiol.*, **31**, 451–461.
57. Balandina,A., Kamashev,D. and Rouviere-Yaniv,J. (2002) The bacterial histone-like protein HU specifically recognizes similar structures in all nucleic acids. DNA, RNA, and their hybrids. *J. Biol. Chem.*, **277**, 27622–27628.
58. Balandina,A., Claret,L., Hengge-Aronis,R. and Rouviere-Yaniv,J. (2001) The *Escherichia coli* histone-like protein HU regulates rpoS translation. *Mol. Microbiol.*, **39**, 1069–1079.
59. Barkan,A. (1989) Tissue-dependent plastid RNA splicing in maize: Transcripts from four plastid genes are predominantly unspliced in leaf meristems and roots. *Plant Cell*, **1**, 437–445.
60. Stahl,D.J., Rodermel,S.R., Bogorad,L. and Subramanian,A.R. (1993) Co-transcription pattern of an introgressed operon in the maize chloroplast genome comprising four ATP synthase subunit genes and the ribosomal *rps2*. *Plant Molec. Biol.*, **21**, 1069–1076.